Table 1
Mean number of water molecules per molecular dynamics frame less than 3 Å from the protonated amine of SG2 and SG12, the phenolic hydroxyl of T1AM, and the carboxylate of SG6 and tafamidis (WAT *OUT*), and from the aniline nitrogen of SG2, SG12, and SG6 and chlorines of tafamidis (WAT *IN*).

	WAT *OUT*	WAT *IN*
SG2	2	0.5
SG12	2.5	0.5
T1AM	1.2	2
SG6	0.02	0.1
Tafamidis	0.03	0

Table 2
Binding free energy of TTR complexes, obtained by the MMPBSA method. VDWAALS = van der Waals contribution; EEL = electrostatic energy; EPB = electrostatic contribution to the solvation free energy calculated by Poisson-Boltzmann method; ENPOLAR = nonpolar solvation free energy contribution; EDISPER = dispersion term; ΔGtot = final estimated binding free energy in kcal/mol.

ENERGY (kcal/mol)	SG2	SG12	T1AM	SG6	Tafamidis
EEL	-28.18	-29.78	-38.44	-30.65	-36.10
WDV	-236.43	-212.91	-241.22	107.02	124.46
EPB	246.31	228.47	260.06	-105.57	-116.50
ENPOLAR	-24.44	-23.53	-26.68	-25.74	-25.71
EDISPER	40.77	39.63	46.96	43.23	45.94
ΔG_{tot}	-1.97	1.87	0.67	-11.72	-7.90

part of the simulation, the main interaction in the inner and outer regions was with water molecules, which was consistent with its relatively weak interaction with TTR. T1AM engaged in fluctuating interactions with K15 by the phenolic OH group (Fig. 7C; magenta line) and a polar interaction between the protonated amine of T1AM and S117 with an average distance of approximately 4 Å (Fig. 7C; gray, distance between heteroatoms), and with T119 (Fig. 7C; orange, distance between heteroatoms). However, in the inner region, the main direct interaction was with water molecules; the distance between the protonated amine of T1AM and the closest water molecules during the simulation was reported to be less than 3 Å (Fig. 7C; cyan). A large number of water molecules seemed to be also attracted in the outer region of the binding site (Fig. 7C; blue). For SG6, strong interactions with S117 and T119 were evident without any water molecule interference or bridges (Fig. 7D). During the simulation a strong interaction was observed between the carboxylate group of SG6 and K15 (alternatively K15 of the A and C chains: the minimum distance is shown in the figure). The interactions with K15, S115, S117, and T119 were maintained, displacing the water that is poorly represented in the binding site. The average number of water molecules per frame of simulation in the region of K15 varies from about 2 for SG2 and SG12, to 1 for T1AM and 0.02 for SG6 (0.03 for tafamidis; see Table 1). Intriguingly, high hydration was detected in the inner region for T1AM, due to its reversed pose placing the protonated amine in this pocket, while no water molecules for tafamidis.

With the aim to validate the binding affinity information suggested by molecular dynamics simulation, a MMPBSA calculation was performed on all complexes (Table 2). In this calculation, T1AM and SG12 complexes showed unfavorable binding energy, and SG2 showed slightly negative energy. On the other hand, SG6 and tafamidis have a favorable free energy, which is in agreement with our experimental results.

Taken together, the results of the MD simulations provide placeable explanation to rationalize the results of the NMR titration experiments and the TTR aggregation assay. An additional effort was made to evaluate the energetic correlation between the NMR data and the closest atoms along the MD trajectory, through a per-residue deconvolution of the interaction energies. The pairwise calculation of the interaction energy between ligands and each binding-site residue is summarized in Fig. 8. No residue in the binding pocket of the SG12-TTR complex was involved in strong interaction with the ligand, except E54. In the T1AM-TTR complex, many residues are involved in weak interactions, covering the central region of the binding site (L17, A108, A109, and L110). Despite the negative term of the electrostatic energy between T1AM and S115, S117, and T119, an unfavorable VDW component led to a slightly positive contribution for the serines, more marked for T119. SG2 seemed, differently, to strongly interact with the central part of the binding site (L17, A108, A109, and L110), and with E54. The latter result was overestimated because the pairwise calculation cannot account for the presence of water, which is crucial for the ionic interaction between E54 and the protonated amine of SG2. Negative values of interaction energy were also detected for the polar residues of the inner region, in agreement with the NMR perturbation results. K15 is involved only in the binding of SG6, with high negative values of energy. For the SG6-TTR complex, the interaction spectrum of the residues is similar to that of SG2, yet with stronger energies. Negative values were detected for L17, A108, A109, L110, S115, S117, and T119.

Notably, molecular dynamics results and energy calculations demonstrate that the presence of a protonated amine, potentially capable to bind E54 analogously to T4, leads to attracting water in the binding site [44]. SG12 lost its initial interaction with S117 and T119; SG2, with the aminoethoxy linker, could engage a strong ionic bond with E54 and retain polar interaction with S115, S117 and T119, but they were substituted by water molecules during the simulation, perhaps due to insufficient chain length. T1AM, despite the high flexibility of the amine chain and its polarity, which could induce a strong interaction with serine residues and T119, attracts stable water molecules in the range of 3 Å from the amine, losing direct contact with the binding site residues.

4. Discussion

The distinct features of thyromimetic molecules in various pathological processes have attracted a wide range of interest. However, despite numerous studies evaluating various beneficial effects of thyromimetics, their interaction with TTR, the TH transporter protein, and the subsequent effects on several TTR-related pathogenic mechanisms,

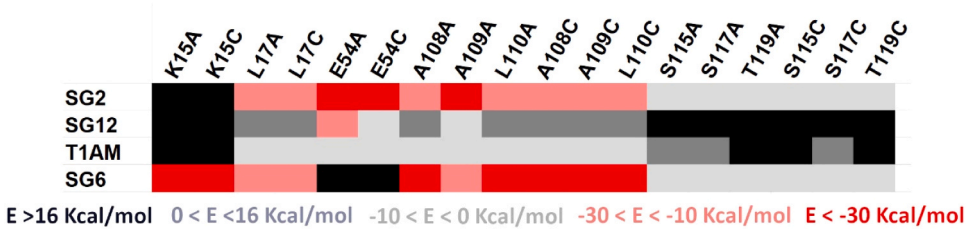

Fig. 8. Results of the pairwise non-bonded energy calculations. The contribution of each residue of the TTR binding site to the ligand stabilization was reported in terms of kcal/mol of interaction energy with the color code labeled as follows: E > 16 kcal/mol colored in black; 0 < E < 16 kcal/mol in dark gray; − 10 < E < 0 kcal/mol in light gray; − 30 < E < −10 kcal/mol in pink; E < −30 kcal/mol in red.

for example, ATTR, have not been sufficiently investigated [45]. To this end, we previously characterized the interaction between TTR and diphenyl-methane-based thyromimetics (sobetirome and its analogs, IS25 and TG68) using NMR spectroscopy and computational simulation, and reported that these molecules interact with and effectively suppress TTR aggregation [46]. In the present study, we aimed to elucidate the binding interaction between TTR and thyronamine-based compounds, including 3-iodothyronamine (T1AM) and its diphenyl-methane analogs (i.e., SG2, SG6, and SG12) and characterize their subsequent effects on TTR aggregation. Although a series of T1AM analogs have been noted as promising therapeutic molecules for obesity and NDDs [11,47], their relationship with TTR has not been elucidated to date.

Our NMR spectroscopic titration experiments confirmed the direct binding of T1AM and its analogs at the hydrophobic T4-binding site of TTR (Fig. 2 and S4). However, subsequent NMR signal perturbation analyses indicated that each T1AM analog exerted differential effects on TTR NMR signals. First, it was evident that the TTR signals were most affected by SG2 and SG6, whereas the effects of T1AM and SG12 were less significant. Moreover, in contrast to the wide signal perturbations by SG2 and SG6 at both the inner and outer regions of the T4-binding pocket, the NMR signal perturbation by T1AM was localized at the outer region, whereas that by SG12 was more focused at the inner region of the binding pocket (Fig. 2). ThT fluorescence and turbidity assay results further corroborated the NMR data (Fig. 3). The activity of T1AM analogs in suppressing acid-induced aggregation of WT TTR was high in the following order: SG6 > SG2 ≈ T1AM > SG12. This correlates well with the NMR signal perturbation (Fig. 2) and intensity change (Fig. S2) results; more significant changes in TTR NMR signals imply a stronger interaction, which subsequently suggests higher stability of the native tetrameric state of TTR.

Intriguingly, the aggregation assays of two pathogenic variants of TTR, V30M and L55P, indicated that the efficacy of T1AM analogs manifests with WT and V30M, not with L55P. This may be attributed to the altered T4 binding site of L55P TTR. Based on our calculation results, E54 play critical roles to stabilize the interaction with T1AM and its analogs. The V30M substitution may cause only, if any, a minimal effect on the binding site architecture, while the effect of L55P substitution would be more significant due to its proximal location to E54. Indeed, the structural model of L55P TTR indicated that the conformation of E54 can be disturbed by the mutation [48]. These observations collectively suggest that a certain TTR variant may require additional consideration for ligand design to ensure its sufficient functionality toward TTR aggregation.

Molecular docking calculations and MD simulation results also provided consistent, yet more detailed explanations for the differential binding interactions of T1AM analogs with TTR. First, the simulation results consistently indicated that SG2 and SG6 were tighter binders of TTR than T1AM and SG12. The intriguing difference in the NMR titration results of SG2 and SG6, however, is that the region including the residues S50-T60 was more affected by the interaction with SG2 than that with SG6. The hints for this came from the simulations suggesting the aminoethoxy chain of SG2 may mediate the interaction with E54, while the carboxylate group of SG6 directly interacts with K15. It is also notable that SG6 exhibited the most inhibitory effects on TTR aggregation, implying the importance of the local interaction between the carboxylate group of the ligand and the amine group of K15 for an aggregation suppressor; a similar observation was made in previous reports that some thyromimetic suppressors of TTR aggregation, such as tafamidis and GC-1 analogs, also contain the terminal carboxylate group that may be involved in the interaction with K15 [21,46]. The simulation results also provide plausible explanations for the NMR signal perturbation results of T1AM and SG12. For T1AM, the computational study predicted the opposite binding and incorporation of water molecules in the region of the T4 binding pocket, resulting in the formation of a complex with reduced stability. The calculations showed SG12 to be a weak binder, mainly due to the lack of a stable interaction network with K15 and E54, in addition to the strong hydration of the amine group. These observations suggest that the single amine moiety of T1AM analogs, in contrast to the single carboxylate, could be critical for the interaction with TTR; they need to have an appropriate linker accommodating the network with K15 and E54, as well as hydrophobic and bulky moieties complementing the inner hydrophobic T4 binding pocket of TTR. Finally, the MMPBSA calculation results summarized these analyses to conclude that the binding affinity of T1AM analogs for TTR is in the following order: SG6 > SG2 > T1AM > SG12, which aligns well with the NMR data and the aggregation assay results.

Taken together, our study provides a novel possibility for using T1AM and its analogs as therapeutic molecules to modulate TTR amyloidosis. Owing to the well-established benefits of TH-derived metabolites and thyromimetics in various human diseases, many related derivatives and analogs have been developed and investigated [2,11,49,50]. In this study, although it was clear that T1AM and its analogs are not as efficient as tafamidis for suppressing the aggregation of TTR, we could still demonstrate that T1AM and its analogs, SG2 and SG6, have therapeutic potentials toward TTR aggregation and prove the feasibility of developing further optimized multi-functional molecules that are effective for both TTR amyloidosis and TH-related metabolic disorders or neurodegeneration.

To the best of our knowledge, this is the first study to observe the direct binding of T1AM and thyronamine-like analogs to TTR. Although a previous study showed that the major transporter of T1AM is apolipoprotein B-100 [51,52], our observations provide a plausible clue that TTR may work as an additional transporter protein at least for some T1AM analogs. This indicates that T1AM analogs may have multiple transport pathways, resulting in differential kinetic profiles and distinctive distributions. Therefore, we believe that the present study may provide novel insights into the working mechanisms of T1AM analogs and how to maximize their efficacies.

Funding

This research was supported by the National Research Foundation funded by the Ministry of Science and ICT, Republic of Korea (grant number NRF-2018R1C1B6008282 to J.H.K.) and the Institute for Basic Science, Republic of Korea (grant number IBS-R007-D1 to Y.H.K). and Pfizer (Project ID: 67562227; J.H.K. and G.C.).

CRediT authorship contribution statement

Bokyung Kim: Conceptualization, Data curation, Investigation, Methodology, Validation, Writing – original draft. **Young Ho Ko**: Data curation, Investigation, Resources. **Jinbeom Si**: Investigation. **Jongbum Na**: Investigation. **Gabriella Ortore**: Conceptualization, Data curation, Investigation, Methodology, Resources, Software, Supervision, Validation, Visualization, Writing – original draft, Writing – review & editing. **Grazia Chiellini**: Conceptualization, Data curation, Funding acquisition, Investigation, Methodology, Resources, Supervision, Validation, Writing – original draft, Writing – review & editing. **Jin Hae Kim**: Conceptualization, Data curation, Funding acquisition, Investigation, Methodology, Resources, Supervision, Validation, Visualization, Writing – original draft, Writing – review & editing.

Declarations of Competing Interest

None.

Acknowledgments

The authors are indebted to Professor Kimoon Kim (Center for Self-assembly and Complexity, Institute for Basic Science) for his considerate support in using the NMR spectrometers. The authors also gratefully acknowledge Prof. Simona Rapposelli (Department of Pharmacy,

University of Pisa) for providing SG-2, SG-6, and SG-12 as a gift.

Appendix A. Supporting information

Supplementary data associated with this article can be found in the online version at doi:10.1016/j.csbj.2023.09.028.

References

[1] Köhrle J, Biebermann H. 3-Iodothyronamine-A thyroid hormone metabolite with distinct target profiles and mode of action. Endocr Rev 2019;40:620–30. https://doi.org/10.1210/er.2018-00182.

[2] Gauthier BR, Sola-García A, Cáliz-Molina MÁ, Lorenzo PI, Cobo-Vuilleumier N, Capilla-González V, et al. Thyroid hormones in diabetes, cancer, and aging. Aging Cell 2020;19:1–25. https://doi.org/10.1111/acel.13260.

[3] Scanlan TS, Suchland KL, Hart ME, Chiellini G, Huang Y, Kruzich PJ, et al. 3-Iodothyronamine is an endogenous and rapid-acting derivative of thyroid hormone. Nat Med 2004;10:638–42. https://doi.org/10.1038/nm1051.

[4] Cöster M, Biebermann H, Schöneberg T, Stäubert C. Evolutionary conservation of 3-iodothyronamine as an agonist at the trace amine-associated receptor 1. Eur Thyroid J 2015;4:9–20. https://doi.org/10.1159/000430839.

[5] Bellusci L, Laurino A, Sabatini M, Sestito S, Lenzi P, Raimondi L, et al. New insights into the potential roles of 3-iodothyronamine (T1AM) and newly developed thyronamine-like TAAR1 agonists in neuroprotection. Front Pharm 2017;8:1–17. https://doi.org/10.3389/fphar.2017.00905.

[6] di Leo N, Moscato S, Borso' M, Sestito S, Polini B, Bandini L, et al. Delivery of thyronamines (Tams) to the brain: a preliminary study. Molecules 2021;26:1616. https://doi.org/10.3390/molecules26061616.

[7] Bellusci L, Runfola M, Carnicelli V, Sestito S, Fulceri F, Santucci F, et al. Endogenous 3-iodothyronamine (T1Am) and synthetic thyronamine-like analog SG-2 act as novel pleiotropic neuroprotective agents through the modulation of SIRT6. Molecules 2020;25:1–14. https://doi.org/10.3390/molecules25051054.

[8] Laurino A, Gencarelli M, Raimondi L. The 3-iodothyronamine (T1AM) and the 3-iodothyroacetic acid (TA1) indicate a novel connection with the histamine system for neuroprotection. Eur J Pharmacol 2021;912:174606. https://doi.org/10.1016/j.ejphar.2021.174606.

[9] Musilli C, De Siena G, Manni ME, Logli A, Landucci E, Zucchi R, et al. Histamine mediates behavioural and metabolic effects of 3-iodothyroacetic acid, an endogenous end product of thyroid hormone metabolism. Br J Pharmacol 2014;171:3476–84. https://doi.org/10.1111/bph.12697.

[10] Chiellini G, Nesi G, Digiacomo M, Malvasi R, Espinoza S, Sabatini M, et al. Design, synthesis, and evaluation of thyronamine analogues as novel potent mouse trace amine associated receptor 1 (m TAAR1) agonists. J Med Chem 2015;58:5096–107. https://doi.org/10.1021/acs.jmedchem.5b00526.

[11] Rutigliano G, Bandini L, Sestito S, Chiellini G. 3-iodothyronamine and derivatives: new allies against metabolic syndrome? Int J Mol Sci 2020;21. https://doi.org/10.3390/ijms21062005.

[12] Bartalena L, Robbins J. Thyroid hormone transport proteins. Clin Lab Med 1993;13:583–98. https://doi.org/10.1016/S0272-2712(18)30427-X.

[13] Hamilton JA, Steinrauf LK, Braden BC, Liepnieks J, Benson MD, Holmgren G, et al. The X-ray crystal structure refinements of normal human transthyretin and the amyloidogenic Val-30 → Met variant to 1.7-Å resolution. J Biol Chem 1993;268:2416–24. https://doi.org/10.1016/s0021-9258(18)53792-3.

[14] Wojtczak A, Cody V, Luft JR, Pangborn W. Structures of human transthyretin complexed with thyroxine at 2.0 Å resolution and 3′,5′-dinitro- N -acetyl- L -thyronine at 2.2 Å resolution. Acta Crystallogr D Biol Crystallogr 1996;52:758–65. https://doi.org/10.1107/S0907444996003046.

[15] Costa PP, Figueira AS, Bravo FR. Amyloid fibril protein related to prealbumin in familial amyloidotic polyneuropathy. Proc Natl Acad Sci USA 1978;75:4499–503. https://doi.org/10.1073/pnas.75.9.4499.

[16] Westermark P, Sletten K, Johansson B, Cornwell GG. Fibril in senile systemic amyloidosis is derived from normal transthyretin. Proc Natl Acad Sci USA 1990;87:2843–5. https://doi.org/10.1073/pnas.87.7.2843.

[17] Johnson SM, Connelly S, Fearns C, Powers ET, Kelly JW. The transthyretin amyloidoses: from delineating the molecular mechanism of aggregation linked to pathology to a regulatory-agency-approved drug. J Mol Biol 2012;421:185–203. https://doi.org/10.1016/j.jmb.2011.12.060.

[18] Grogan M, Scott CG, Kyle RA, Zeldenrust SR, Gertz MA, Lin G, et al. Natural history of wild-type transthyretin cardiac amyloidosis and risk stratification using a novel staging system. J Am Coll Cardiol 2016;68:1014–20. https://doi.org/10.1016/j.jacc.2016.06.033.

[19] Si JB, Kim B, Kim JH. Transthyretin misfolding, a fatal structural pathogenesis mechanism. Int J Mol Sci 2021;22. https://doi.org/10.3390/ijms22094429.

[20] Miroy GJ, Lai Z, Lashuel HA, Peterson SA, Strang C, Kelly JW. Inhibiting transthyretin amyloid fibril formation via protein stabilization. Proc Natl Acad Sci USA 1996;93:15051–6. https://doi.org/10.1073/pnas.93.26.15051.

[21] Bulawa CE, Connelly S, DeVit M, Wang L, Weigel C, Fleming JA, et al. Tafamidis, a potent and selective transthyretin kinetic stabilizer that inhibits the amyloid cascade. Proc Natl Acad Sci USA 2012;109:9629–34. https://doi.org/10.1073/pnas.1121005109.

[22] Maurer MS, Schwartz JH, Gundapaneni B, Elliott PM, Merlini G, Waddington-Cruz M, et al. Tafamidis treatment for patients with transthyretin amyloid cardiomyopathy. N Eng J Med 2018;379:1007–16. https://doi.org/10.1056/nejmoa1805689.

[23] Casal I, Monteiro S, Beirão JM. Tafamidis in hereditary ATTR amyloidosis – our experience on monitoring the ocular manifestations. Amyloid 2016;23:262–3. https://doi.org/10.1080/13506129.2016.1236332.

[24] Salvi F, Volpe R, Pastorelli F, Bianchi A, Vella A, Rapezzi C, et al. Failure of tafamidis to halt progression of Ala36Pro TTR oculomeningovascular amyloidosis. J Stroke Cereb Dis 2018;27:e212–4. https://doi.org/10.1016/j.jstrokecerebrovasdis.2018.04.033.

[25] Kim JH, Oroz J, Zweckstetter M. Structure of monomeric transthyretin carrying the clinically important T119M mutation. Angew Chem Int Ed 2016;55:16168–71. https://doi.org/10.1002/anie.201608516.

[26] Liu K, Kelly JW, Wemmer DE. Native state hydrogen exchange study of suppressor and pathogenic variants of transthyretin. J Mol Biol 2002;320:821–32. https://doi.org/10.1016/S0022-2836(02)00471-0.

[27] Leach BI, Zhang X, Kelly JW, Dyson HJ, Wright PE. NMR measurements reveal the structural basis of transthyretin destabilization by pathogenic mutations. Biochemistry 2018;57:4421–30. https://doi.org/10.1021/acs.biochem.8b00642.

[28] Lee W, Rahimi M, Lee Y, Chiu A. POKY: a software suite for multidimensional NMR and 3D structure calculation of biomolecules. Bioinformatics 2021;37:3041–2. https://doi.org/10.1093/bioinformatics/btab180.

[29] Lai Z, Colón W, Kelly JW. The acid-mediated denaturation pathway of transthyretin yields a conformational intermediate that can self-assemble into amyloid. Biochemistry 1996;35:6470–82. https://doi.org/10.1021/bi952501g.

[30] Robinson LZ, Reixach N. Quantification of quaternary structure stability in aggregation-prone proteins under physiological conditions: the transthyretin case. Biochemistry 2014;53:6496–510. https://doi.org/10.1021/bi500739q.

[31] Berman HM, Westbrook J, Feng Z, Gilliland G, Bhat TN, Weissig H, et al. The protein data bank. Nucleic Acids Res 2000;28:235–42.

[32] Ortore G, Martinelli A. Identification of transthyretin fibril formation inhibitors using structure-based virtual screening. ChemMedChem 2017;12:1327–34. https://doi.org/10.1002/cmdc.201700051.

[33] D.A. Case, R.M. Betz, D.S. Cerutti, T.E. Cheatham, III, T.A. Darden, R.E. Duke, T.J. Giese HG, A.W. Goetz, N. Homeyer, S. Izadi, P. Janowski, J. Kaus, A. Kovalenko, T. S. Lee, S. LeGrand, P. Li C., Lin, T. Luchko, R. Luo, B. Madej, D. Mermelstein, K.M. Merz, G. Monard, H. Nguyen, H.T. Nguyen I., Omelyan, A. Onufriev, D.R. Roe, A. Roitberg, C. Sagui, C.L. Simmerling, W.M. Botello-Smith JS, R.C. Walker, J. Wang, R.M. Wolf, X. Wu LX and P.A.K.. AMBER 2016, University of California, San Francisco 2016.

[34] Roe DR, Cheatham TE. PTRAJ and CPPTRAJ: software for processing and analysis of molecular dynamics trajectory data. J Chem Theory Comput 2013;9:3084–95. https://doi.org/10.1021/ct400341p.

[35] Pettersen E, Goddard T, Huang C, Couch G, Greenblatt D, Meng E, et al. UCSF Chimera – a visualization system for exploratory research and analysis. J Comput Chem 2004;25:1605–12. https://doi.org/10.1002/jcc.20084.

[36] Wang C, Nguyen PH, Pham K, Huynh D, Le TBN, Wang H, et al. Calculating protein-ligand binding affinities with MMPBSA: method and error analysis. J Comput Chem 2016;37:2436–46. https://doi.org/10.1002/jcc.24467.

[37] Miller BR, McGee TD, Swails JM, Homeyer N, Gohlke H, Roitberg AE. MMPBSA.py: An efficient program for end-state free energy calculations. J Chem Theory Comput 2012;8:3314–21. https://doi.org/10.1021/ct300418h.

[38] Colon W, Kelly JW. Partial denaturation of transthyretin is sufficient for amyloid fibril formation in vitro. Biochemistry 1992;31:8654–60. https://doi.org/10.1021/bi00151a036.

[39] Jacobson DR, McFarlin DE, Kane I, Buxbaum JN. Transthyretin Pro 55, a variant associated with early-onset, aggressive, diffuse amyloidosis with cardiac and neurologic involvement. Hum Genet 1992;89:353–6.

[40] Jacobson DR, Buxbaum JN. Genetic aspects of amyloidosis. Adv Hum Genet 1991;20:69–123.

[41] Cotrina EY, Santos LM, Rivas J, Blasi D, Leite JP, Liz MA, et al. Targeting transthyretin in Alzheimer's disease: drug discovery of small-molecule chaperones as disease-modifying drug candidates for Alzheimer's disease. Eur J Med Chem 2021;226:113847. https://doi.org/10.1016/j.ejmech.2021.113847.

[42] Mizuguchi M, Yokoyama T, Okada T, Nakagawa Y, Fujii K, Nabeshima Y, et al. Benziodarone and 6-hydroxybenziodarone are potent and selective inhibitors of transthyretin amyloidogenesis. Bioorg Med Chem 2023;90. https://doi.org/10.1016/j.bmc.2023.117370.

[43] Haupt M, Blakeley MP, Fisher SJ, Mason SA, Cooper JB, Mitchell EP, et al. Binding site asymmetry in human transthyretin: insights from a joint neutron and X-ray crystallographic analysis using perdeuterated protein. IUCrJ 2014;1:429–38. https://doi.org/10.1107/S2052252514021113.

[44] Liu D, Wyttenbach T, Bowers MT. Hydration of protonated primary amines: effects of intermolecular and intramolecular hydrogen bonds. Int J Mass Spectrom 2004;236:81–90. https://doi.org/10.1016/J.IJMS.2004.05.013.

[45] Saponaro F, Kim JH, Chiellini G. Transthyretin stabilization: an emerging strategy for the treatment of alzheimer's disease? Int J Mol Sci 2020;21:1–13. https://doi.org/10.3390/ijms21228672.

[46] Kim B, Ko YH, Runfola M, Rapposelli S, Ortore G, Chiellini G, et al. Diphenylmethane based thyromimetic inhibitors for transthyretin amyloidosis. Int J Mol Sci 2021;22. https://doi.org/10.3390/ijms22073488.

[47] Runfola M, Perni M, Yang X, Marchese M, Bacci A, Mero S, et al. Identification of a thyroid hormone derivative as a pleiotropic agent for the treatment of Alzheimer's disease. Pharmaceuticals 2021;14. https://doi.org/10.3390/ph14121330.

[48] Saelices L, Johnson LM, Liang WY, Sawaya MR, Cascio D, Ruchala P, et al. Uncovering the mechanism of aggregation of human transthyretin. J Biol Chem 2015;290:28932–43. https://doi.org/10.1074/jbc.M115.659912.

[49] Brenta G, Danzi S, Klein I. Potential therapeutic applications of thyroid hormone analogs. Nat Clin Pract Endocrinol Metab 2007;3:632–40. https://doi.org/10.1038/ncpendmet0590.
[50] Zucchi R. Thyroid hormone analogues: an update. Thyroid 2020;30:1099–105. https://doi.org/10.1089/thy.2020.0071.
[51] Roy G, Placzek E, Scanlan TS. ApoB-100-containing lipoproteins are major carriers of 3-iodothyronamine in circulation. J Biol Chem 2012;287:1790–800. https://doi.org/10.1074/jbc.M111.275552.
[52] Janssen ST, Janssen OE. Directional thyroid hormone distribution via the blood stream to target sites. Mol Cell Endocrinol 2017;458:16–21. https://doi.org/10.1016/j.mce.2017.02.037.